A concept of dual-salt polyvalent-metal storage battery

Shunsuke Yagi,[1] Tetsu Ichitsubo,[2,*] Yoshimasa Shirai,[2] Shingo Yanai,[2] Takayuki Doi,[3]
Kuniaki Murase,[2] Eiichiro Matsubara[2]
[1] *Nanoscience and Nanotechnology Research Center, Osaka Prefecture University, Osaka 599-8570, Japan*
[2] *Department of Materials Science and Engineering, Kyoto University, Kyoto 606-8501, Japan*
[3] *Department of Molecular Chemistry and Biochemistry, Doshisha University, Kyotanabe, Kyoto 610-0321, Japan*
[*] *Corresponding author: tichi@mtl.kyoto-u.ac.jp*
(Dated: October 29, 2013)

In this work, we propose and examine a battery system with a new design concept. The battery consists of a non-noble polyvalent metal (such as Ca, Mg, Al) combined with positive electrode already well-established for lithium ion batteries (LIBs). The prototype demonstrated here is composed of a Mg negative electrode, $LiFePO_4$ positive electrode, and tetrahydrofuran solution of two kinds of salts ($LiBF_4$ and phenylmagnesium chloride) as an electrolyte. The LIB positive-electrode materials such as $LiFePO_4$ can preferentially accommodate Li^+ ions; i.e., they work as a "Li pass filter". This characteristic enables us to construct a septum-free, Daniel-battery type dual-salt polyvalent-metal storage battery (PSB). The presented dual-salt PSB combines many advantages, *e.g.*, fast diffusion of Li^+ ions in the positive electrode, high cyclability, and high specific capacity of lightweight polyvalent metals. The concept is expected to allow the design of many combinations of dual-salt PSBs having high energy density and high rate capability.

1. INTRODUCTION

High energy-density and affordable batteries that can store surplus electric power, so-called rechargeable storage batteries, are strongly demandedfrom the viewpoint of energy and environmental problems. Recently, lithium ion batteries (LIBs) have been widely used as storage batteries. If lithium metal could be used as the negative electrode instead of graphite or other carbonaceous materials, LIBs would show considerably high energy density, but this is not possible due to its dendritic growth during charge.[1] As a result, the high potential of LIBs cannot currently be exploited to its maximum. Thus, new innovative battery systems are required to enhance energy density for future electric vehicles and other large-scale affordable storage battery systems that are demanded for future smart-grid societies.

In recent years, non-noble metals (such as Ca, Mg, Al etc) which yield polyvalent cations have been highly expected to be applicable as negative electrode materials for future polyvalent-metal storage batteries (PSBs). Magnesium metal has been attracting particularly significant attention, not only for its low standard electrode potential (−2.36 V vs SHE)[2,3] and large theoretical capacity (2234 mAh g^{-1}), but also for its safer handling, abundance, and inexpensiveness. However, there are many problems to be overcome for the realization of such PSBs, including magnesium storage batteries (MSBs). It is known that the electrodeposition of polyvalent cations via desolvation is fundamentally difficult, and their topotactic motion is quite sluggish due to strong coulomb restraint.

The path to the realization of MSBs was opened up by the trailblazing work of Aurbach et al. in 2000[4], since which MSBs have been investigated systematically.[5–10] These battery systems consist of a Mg-metal negative electrode, Chevrel-compound ($Mg_2Mo_6S_8$ etc) positive electrode, and a Grignard reagent (RMgX, R: Alkyl or aryl group, X: halogen)[11] and $AlX_{3-x}R_x$ salt in the tetrahydrofuran (THF) solvent. The salient result was the successful demonstration of prototype MSBs that had been previously regarded as a quite unfeasible battery technology. While other candidate positive-electrode materials for MSBs have been reported,[12,13] currently only Chevrel compounds show superior intercalation/deintercalation characteristics as a potential positive electrode material. However, even when Chevrel compounds are used as the positive electrode in MSBs, MSBs deliver lower voltages (about 1.1–1.2 V for $Mg_2Mo_6S_8$)[4,14,15] than the typical LIB cell voltage (about 4–5 V),[16] and, in addition, the diffusion of the polyvalent cations is rather slower than the diffusion of Li^+ in LIBs, resulting in a lower electric power (i.e., rate capability).

Thus, in comparison with LIB research, MSB research is limited by the few choices in positive electrode and electrolyte combinations available. Nevertheless, the development of MSBs is greatly expected; unlike Li metal, Mg metal can be used as a negative electrode, because it can be electrodeposited rather smoothly without dendritic growth.[16–19] The use of Mg metal as a negative electrode would enhance battery capacity in comparison with graphite (about 370 mAh g^{-1}); this would improve energy density by up to about 4–5 times from only the standpoint of the negative electrode, although the electromotive force (*Emf*) would be decreased by about 0.4–0.7 V compared with that of LIBs (see SI Table I).

In this work, we present a new concept for the development of PSBs, in which positive electrodes commonly used for LIBs are employed in combination with polyvalent metals. We devise a dual-salt (Li salt and Mg/Ca/Al salt) electrolyte to improve the performance of the LIB positive electrode for PSB systems. Our concept exploits the characteristics of the LIB positive electrodes to preferentially accommodate Li^+ ions prior to the polyvalent cations (Mg^{2+}, Ca^{2+}, Al^{3+}). We will thereby obtain the following advantages: (1) The *Emf* of the proposed PSBs can be easily tailored, and in principle high-voltage batteries of 3–4V can be designed. (2) Electric power comparable to that of LIBs. (3) Many kinds of PSBs can be designed, provided an appropriate electrolyte is available.

2. DUAL-SALT BATTERY CONCEPT

A new concept for the realization of PSBs on the basis of the classical Daniel battery is illustrated in Fig. 1. As seen in Fig. 1a, the classical Daniel battery uses a septum to separate the two kinds of cations and to prevent the displacement deposition of a more noble metal (Cu) on the less-noble electrode (Zn). However, the presence of this septum makes production of the battery laborious. The proposed PSBs, shown in Fig. 1b, use a LIB positive electrode material (*e.g.*, $LiFePO_4$ or $LiCoO_2$, etc) is employed and a non-noble polyvalent metal (other than Li) negative electrode, and both kinds of cations are dissolved in the same solvent without a septum. Because Li^+ ions are the most non-noble in the supposed battery system, other non-noble metals such as Ca, Mg, and Al can be used as the negative-electrode material because Li metal will not be deposited onto them. In addition, such polyvalent cations (Ca^{2+}, Mg^{2+}, Al^{3+}) are preferentially electrodeposited over Li^+ ions during charge. In the positive electrode, Li^+ ions are deintercalated from the host during charge, and only Li^+ ions are intercalated into the host during discharge, because it is quite difficult for the polyvalent cations to intercalated into the host. Thus, the host compound for the LIB positive electrode plays the role of a "Li pass filter" during discharge, and the electrodeposition of Li can be electrochemically controlled during charge. Therefore, a septum is not required for this battery system. As shown in Fig. 1c, there are many possible combinations of positive and negative electrode materials with which PSB can be composed, and the resulting PSBs can deliver various *Emf* values according to the combination chosen.[20,21]

In the present work, we demonstrate a prototype PSB using $LiFePO_4/FePO_4$ (LFP/FP) as a positive electrode,[22] Mg as a negative electrode, and a tetrahydrofuran solution of two different kinds of salts ($LiBF_4$ and phenylmagnesium chloride) as an electrolyte. The reasons why these two electrodes were chosen are as follows: (i) The electrolyte and solvent are already established for MSBs,[4,11] (ii) the electrochemical window of the Grignard-reagent/THF electrolyte is about 2–3 V (not so wide), and $LiFePO_4$ which has a lower electrode potential (3.4 V vs Li/Li^+) is therefore appropriate for the demonstration, (iii) $LiFePO_4$ shows excellent cyclability (more than 700 cycles for $LiFePO_4$).[23] In the dual-salt PSB system chosen, the following redox half-cell reactions would occur at the positive electrode (PE) and negative electrode (NE) during discharge, respectively:

$$\begin{aligned} \text{PE}: &\quad FePO_4 + Li^+ + e^- \rightarrow LiFePO_4 \\ \text{NE}: &\quad Mg \rightarrow Mg^{2+} + 2e^- \\ \text{Total}: &\quad FePO_4 + Li^+ + \frac{1}{2}Mg \rightarrow LiFePO_4 + \frac{1}{2}Mg^{2+} \end{aligned}$$

where the phase separation phenomenon[24] in $LiFePO_4$ is neglected in the equation.

3. EXPERIMENTAL

Commercially available $LiFePO_4$ (Tatung fine chemicals Co., Ltd., Taiwan, BET surface: 9.97 m^2 g^{-1}) was used as the active material for the positive electrode, and magnesium ribbon (Nilaco Co., Ltd., Japan) was used as the negative electrode and reference electrode. The electrolyte for the dual-salt PSB, a THF solution containing 1.00 M phenylmagnesium chloride (PhMgCl), 0.20 M $LiBF_4$, and 0.20 M $AlCl_3$ was prepared by dissolving PhMgCl (2 M solution in THF, Sigma-Aldrich, USA), $LiBF_4$ (Nacalai Tesque, Inc., Japan), and $AlCl_3$ (Nacalai Tesque, Inc.) in THF (Sigma-Aldrich) in a glove box filled with Ar gas of a dew point of about -70°C. The electrolyte composition used for comparative experiments was 0.50 M PhMgCl and 0.25 M $AlCl_3$ in THF, which was determined according to previous data.[7,18,19] The strong Lewis acid $AlCl_3$ was added for the transmetalation reaction to effectively yield $MgCl^+$ complex ions.[7] Each composite positive electrode was prepared by coating a Pt plate with a mixture of $LiFePO_4$ (active material), carbon black (super C 65, as conductive agents), and PVdF (binder) in a weight percent ratio of 8:1:1. Electrochemical measurements were carried out in the glove box in beaker cells with the three electrode setup, using a potentiostat (SP-200 or VMP3, Bio-Logic SAS, France). The crystalline structures of the active materials were analyzed by X-ray diffraction (XRD: RIGAKU Co., Japan, SmartLab) with Cu$K\alpha$ or Cr$K\alpha$ radiation. The

surface morphology of the precipitate was observed by scanning electron microscopy (SEM; JSM-6010LA, JEOL Ltd., Japan). The crystal structures in the presented figures were drawn using VESTA 3 software.[25]

4. RESULTS AND DISCUSSION

Figure 2 shows cyclic voltammograms obtained in (a) THF electrolyte containing 0.50 M PhMgCl and 0.25 M $AlCl_3$, (b) and (c) THF electrolyte containing 1.0 M PhMgCl, 0.20 M$AlCl_3$, and 0.20 M $LiBF_4$. The cyclic voltammogram in Fig. 2(a) was obtained for almost delithiated LFP in the electrolyte containing no lithium salt. The absence of a cathodic peak and the significantly low cathodic current suggest that Mg^{2+} ions are difficult to intercalate into the $FePO_4$ (FP) host. In contrast, a cathodic peak in addition to an anodic peak were clearly observed in the electrolyte containing sufficient Li^+ ions (Fig. 2(b)). Thus, Li^+ ions were preferentially intercalated into the FP host structure, which means that the FP structure played a significant role as a Li pass filter, as expected above. Conversely, a large cathodic current was observed below about 0 V vs. Mg when Pt electrode was used as the working electrode (Fig. 2(c)). Fig. 3 shows the SEM images and XRD profiles of the deposits obtained at -0.5 V and -1.5 V vs. Mg (electrical charge: 3 C cm^{-2}). As shown in Fig. 3, the deposits were smooth and flat Mg(-Li) metal(alloy), especially even though the latter potential (-1.5V vs. Mg) is considered to be below the electrodeposition potential of Li. Thus, the Mg(-Li) deposits were not dendritic and Mg(-Li) metal(alloy) is therefore useable as an active material for high specific-capacity negative electrodes.

We conducted battery tests besed on the cyclic voltammetry results. Due to the narrow electrochemical-window concern (about 2.4 V vs. Mg as shown in Fig. 2(c)), limited charge/discharge tests (charged electricity amount: 60 mAh g^{-1}) were performed to reduce the effect of electrolyte decomposition. Prior to the discharge test, the $LiFePO_4$ (LFP) active material was sufficiently delithiated in a conventional LIB electrolyte, 1.0 M $LiPF_6$/ethylene carbonate-dimethyl carbonate in 1:2 volume ratio. Figure 4(a) shows the discharge/charge behaviors in the dual-salt electrolyte. The plateau voltage of about 2.3 V during discharge was characterized by the two phase reaction of LFP/FP, and the value of the counter-electrode (CE) potential was in the potential region of the anodic dissolution of Mg. Next, the battery test was begun from the charge process with a more concentrated $LiBF_4$ solute (0.40 M) in the electrolyte. As seen in Fig. 4(b), the battery could be charged and discharged as well in the case of 0.20 M $LiBF_4$ electrolyte. In both cases, however, the extra electrical charge due to anodic decomposition of the electrolyte was consumed during charge and, hence, the active material was discharged up to about half of the charged electricity (about 30 mAh g^{-1}). Fig. 5 shows discharge-charge curves during 2 cycles at 1/10 C using $FePO_4$ formed by charge in the conventional electrolyte for LIBs; the discharge process was first performed in the dual-salt electrolyte. The discharge capacity at the 1st cycle was about 124 mAh g^{-1}. The missing capacity, *i.e.* 46 mAh g^{-1}, is attributed to the self-discharge of $FePO_4$ along with the electrolyte decomposition. After the charge up to 170 mAh g^{-1} in the dual-salt electrolyte, the discharge capacity (2nd cycle) was about 96 mAh g^{-1} The reason of the missing capacity, *i.e.* 74 mAh g^{-1}, is the electrolyte decomposition during charge in addition to the self-discharge. However, the battery could be charged and discharged also in this case. It was further found that the battery could be fully charged and discharged in the dual-salt electrolyte with 0.20 M $LiBF_4$. Fig. 6 shows X-ray diffraction (XRD) profiles obtained after sufficient charge and discharge processes in the dual-salt electrolyte; Fig. 6(a), measured after full charge (accompanied by anodic decomposition of the electrolyte), and Fig. 6(b), measured after fully discharging the fully charged cell. It was confirmed that the LFP phase was changed to the FP phase after charge and that FP was transformed to LFP after discharge.

Thus, the present dual-salt battery concept was shown to work well, as demonstrated experimentally. The idea of a "Li pass filter" used in this battery concept is itself scientifically interesting, but two issues must be overcome for practical application. One is the instability of the electrolyte. The electrolyte proposed here contains dissolved $LiBF_4$ and PhMgCl; there is a possibility that BF_4^- would react with PhMgCl to give $B(Ph)_4^-$, which might lower the stability of the electrolyte. The other issue is that all carrier ions (all Mg^{2+} ions after discharge and all Li^+ ions after charge) have to be accommodated in the electrolyte in this battery system, which means a large amount of electrolyte solvent is required. If the amount of electrolyte can be reduced to be comparable to that of conventional LIBs, the energy density of the present dual-salt PSBs would be significantly enhanced and they would be more widely applicable for various fields such as electric vehicles. We are trying to solve this issue by using a saturated electrolyte, where the precipitated salts work as a reservoir and source of the carrier cations to decrease the amount of the electrolyte required. The energy densities of the dual-salt PSBs are expected to be almost comparable to those of the LIBs on the assumption that Li salt, existing as a precipitates in the small amount of a saturated electrolyte, works as a Li^+ ion reservoir (See SI Table I); this will be reported in detail as a future work.

5. CONCLUSIONS

We have presented a new design concept of dual-salt Daniel type PSBs, which will provide various types of battery systems. Considering the LIB field, the advantageous points obtained by substituting them for the conventional graphite negative electrode would be as follows: (1) facile redox reactions at the negative electrode owing to a simple anodic dissolution and cathodic electrodeposition of the metal, (2) high cyclability without any intercalation into the active material, (3) savings in the cell volume and weight due to the metal negative electrodes being free from metallic current collector and binder, (4) simple fabrication of the metal negative electrode (placement of metal foil without production of a composite material consisting of binder and active material), (5) lower irreversible capacity (graphite has a large irreversible capacity at a high redox potential). In comparison with the Mg battery, the following are advantages: (6) higher energy density, (7) a facile reaction at the positive electrode due to elimination of the sluggish diffusion process of the polyvalent Mg^{2+} cations in a solid active material, leading to a higher power density. Finally, from the standpoints of the element strategy where no Li element is used, the combination of the positive electrode for the Na battery with a Mg (or Ca or Al) negative electrode may be attractive for future development.

For future practical application, it will be indispensable to develop appropriate electrolytes with a wider electrochemical potential window. Furthermore, it is necessary to overcome the drawback of the considerable amount of electrolyte required in the proposed PSBs.

Acknowledgements

We are grateful to Mr. Akira Tanaka and Mr. Yuya Ichikawa from Osaka Prefecture University for their help in confirming the reproducibility of the experimental results. One of the authors, T.I., is grateful to Professor Yoshitaro Nose, Kyoto University, for valuable discussions. This work was supported in part by the Advanced Low Carbon Technology Research and Development Program (ALCA) and by a Grant-in-Aid from the Special Coordination Funds for Promoting Science and Technology commissioned by JST, MEXT of Japan.

[1] J. -M. Tarascon, & M. Armand, *Nature* **414**, 359-367 (2001).
[2] W. M. Latimer, in *The oxidation states of the elements and their potentials in aqueous solutions, 2nd ed.* (Prentice-hall, INC. Englewood Cliffs, N. J. 1959).
[3] M. Pourbaix, in *Atlas of electrochemical equilibria in aqueous solutions* (Cebelcor, Brüssel, 1966).
[4] D. Aurbach, Z. Lu, A. Schechter, Y. Gofer, H. Gizbar, R. Turgeman, Y. Cohen, M. Moshkovich, & E. Levi, *Nature* **407**, 724-727 (2000).
[5] D. Aurbach, G. S. Suresh, E. Levi, A. Mitelman, O. Mizrahi, O. Chusid, & M. Brunelli, Adv. Mater. **19**, 4260-4267 (2007).
[6] N. Amir, Y. Vestfrid, O. Chusid, Y. Gofer, & D. Aurbach, *J. Power Sources* **174**, 1234-1240 (2007).
[7] O. Mizrahi, N. Amir, E. Pollak, O. Chusid, V. Marks, H. Gottlieb, L. Larush, E. Zinigrad, & D. Aurbach, *J. Electrochem. Soc.* **155**(2), A103-A109 (2008).
[8] E. Levi, M.D. Levi, O. Chasid, & D. Aurbach, *J. Electroceram.* **22**, 13-19 (2009).
[9] E. Levi, Y. Gofer, & D. Aurbach, *Chem. Mater.* **22**, 860-868 (2010).
[10] S.F. Amalraj, & D. Aurbach, *J. Solid State Electrochem.* **15**, 877-890 (2011).
[11] C. Liebenow, *J. Appl. Electrochem.* **27**(2), 221-225 (1997).
[12] P. Novák, & J. Desilvestro, *J. Electrochm. Soc.* **140**(1), 140-144 (1993).
[13] T. Ichitsubo, T. Adachi, S. Yagi, & T. Doi, *J. Mater. Chem.* **21**, 11764-11772 (2011).
[14] T.D. Gregory, R.J. Hoffman, & R. Winterton, **137**(3), 775-780 (1990).
[15] M. Morita, N. Yoshimoto, S. Yakushiji, & M. Ishikawa, **4**(11), A177-A179 (2001).
[16] J.O. Besenhard, & M. Winter, *Chem. Phys. Chem.* **3**(2), 155-159 (2002).
[17] M. Matsui, *J. Power Sources* **196**, 7048-7055 (2011).
[18] S. Yagi, A. Tanaka, T. Ichitsubo, & E. Matsubara, *ECS Electrochem Lett.* **1**(2), D11-D14 (2012)
[19] S. Yagi, A. Tanaka, Y. Ichikawa, T. Ichitsubo, & E. Matsubara, *J. Electrochem. Soc.* **160**(3), C83-C88 (2013).
[20] J.B. Goodenough, & Y. Kim, *Chem. Mater.* **22**(3), 587-603 (2010).
[21] M. Nagahama, N. Hasegawa, & S. Okada, *J. Electrochem. Soc.* **157**(6), A748-A752 (2010).
[22] A.K. Padhi, K.S. Nanjundaswamym, & J.B. Goodenough, *J. Electrochem. Soc.* **144**, 1188-1194 (1997).
[23] P.P Prosini, M. Carewska, S. Scaccia, P. Wisniewski, & M. Pasquali, *Electrochim. Acta* **48**(28), 4205-4211 (2003).
[24] T. Ichitsubo, K. Tokuda, S. Yagi, M. Kawamori, T. Kawaguchi, T. Doi, M. Oishi, & E. Matsubara, *J. Mater. Chem. A* **1**, 2567-2577 (2013).
[25] K. Momma, & F. Izumi, *J. Appl. Crystallogr.* **44**, 1272-1276 (2011).

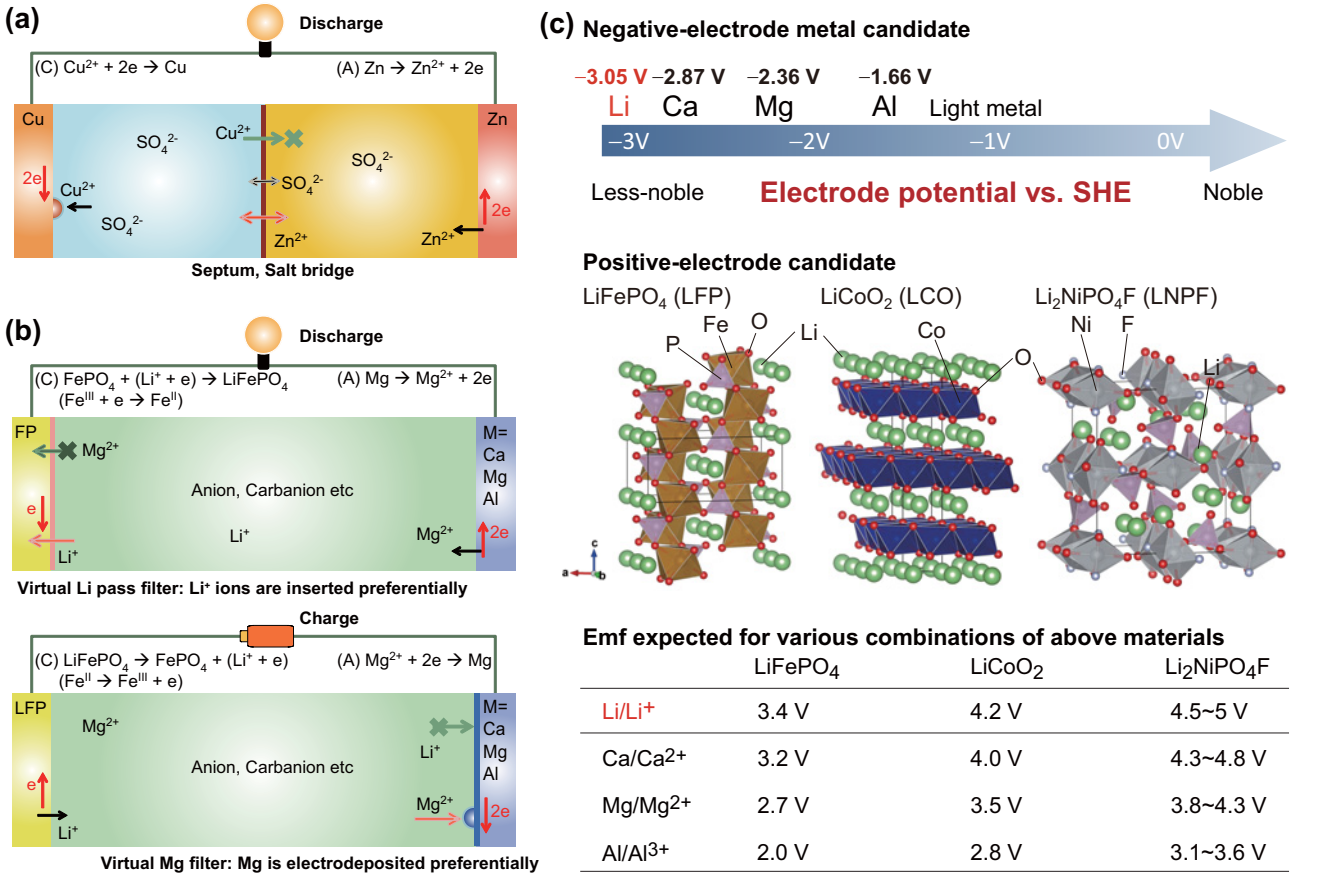

Emf expected for various combinations of above materials

	$LiFePO_4$	$LiCoO_2$	Li_2NiPO_4F
Li/Li^+	3.4 V	4.2 V	4.5~5 V
Ca/Ca^{2+}	3.2 V	4.0 V	4.3~4.8 V
Mg/Mg^{2+}	2.7 V	3.5 V	3.8~4.3 V
Al/Al^{3+}	2.0 V	2.8 V	3.1~3.6 V

FIG. 1: A concept for dual-salt PSBs. (a) Schematic illustration of the classical Daniel battery. (b) Schematic illustration of the septum-free PSB based on the Daniel battery. In these figures, the case of M = Mg is illustrated as an example. (c) Examples of negative and positive electrode materials for the proposed PSBs, and expected *Emf* values for various electrode material combinations on the basis of the literature data.[2,3,20,21]

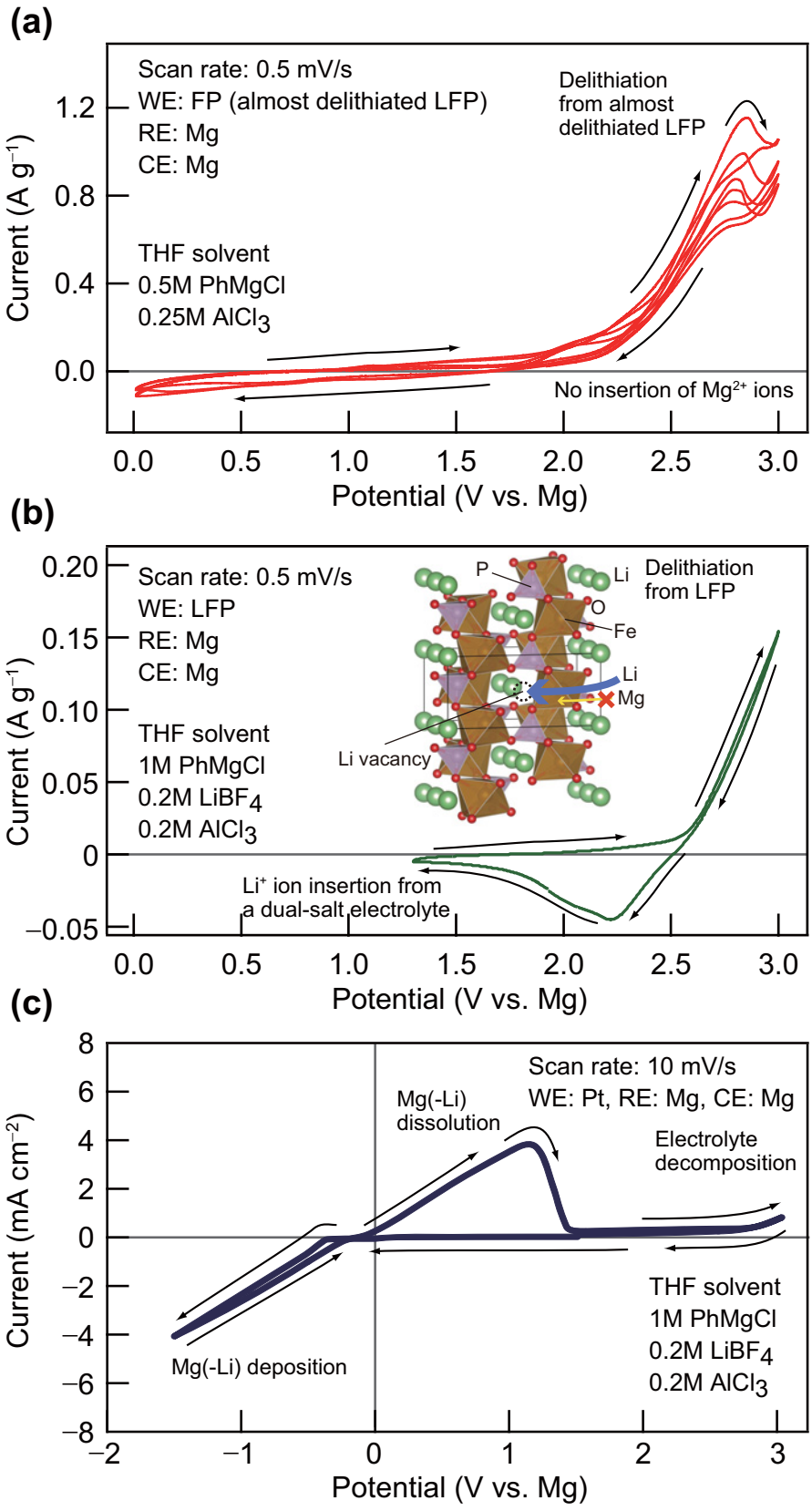

FIG. 2: Cyclic voltammograms obtained in (a) THF electrolyte containing PhMgCl and $AlCl_3$, (b) and (c) THF electrolyte containing PhMgCl, $LiBF_4$, and $AlCl_3$ using (a)$FePO_4$ (almost delithiated $LiFePO_4$), (b) $FePO_4$/$LiFePO_4$, and (c) Pt as the working electrode.

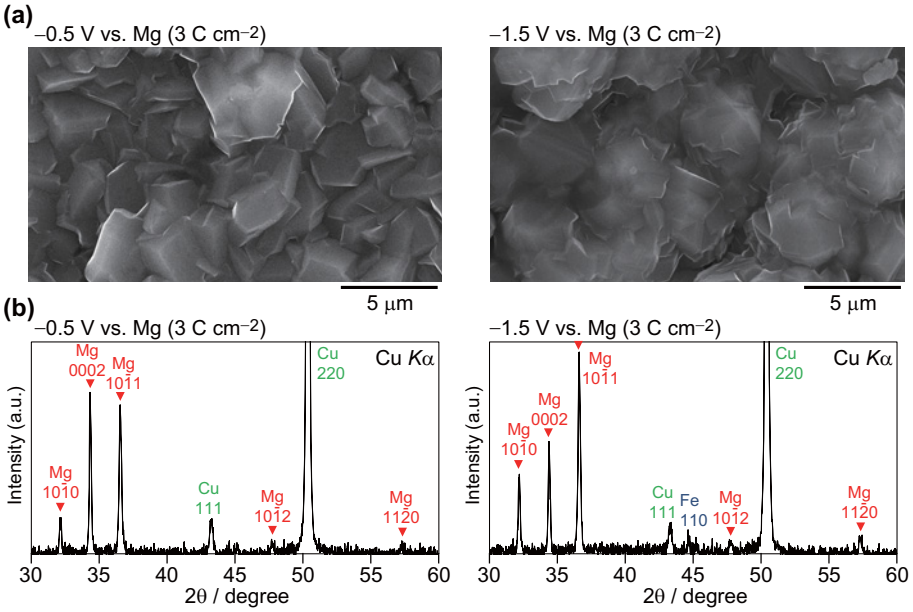

FIG. 3: (a) SEM images and (b) XRD profiles of the deposit obtained at −0.5 and −1.5 V vs. Mg (electrical charge: 3 C cm^{-2}). Peaks due to Cu and Fe correspond to Cu foil(substrate) and the stage, respectively.

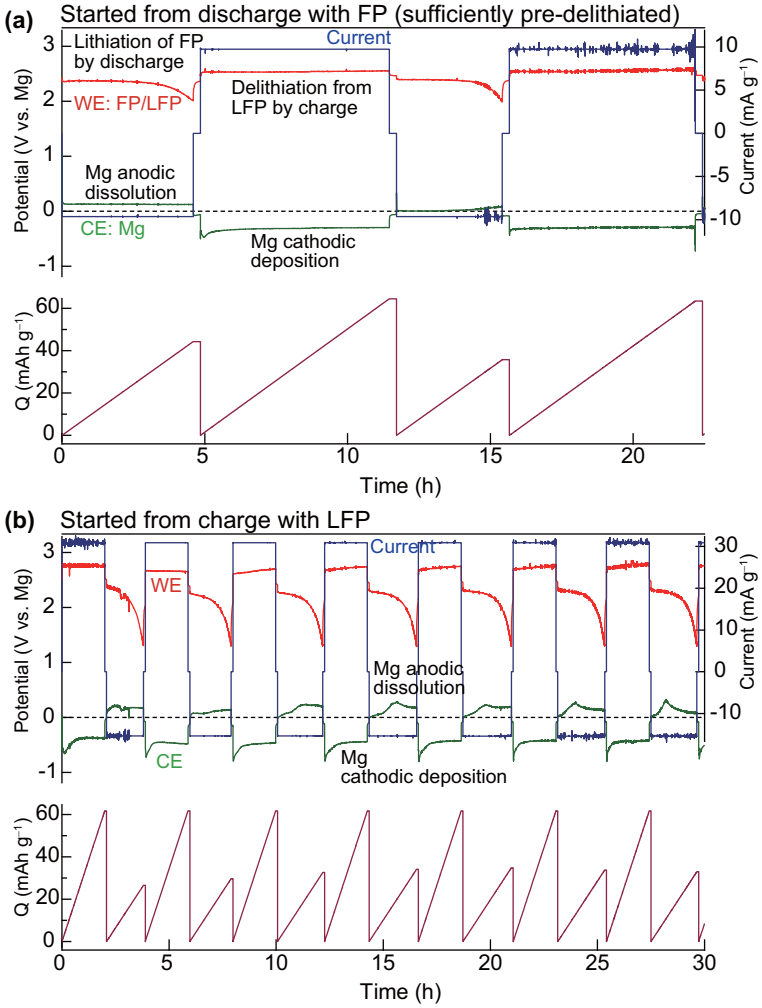

FIG. 4: Charge-discharge performance of the PSB using (a) sufficiently pre-delithiated $LiFePO_4$ and (b) non-treated $LiFePO_4$. Cutoff voltage: (a)2.0, and (b)1.3 V for discharge, (a,b) 2.8 V for charge or charged electricity amount Q, 60 mAh g^{-1}.

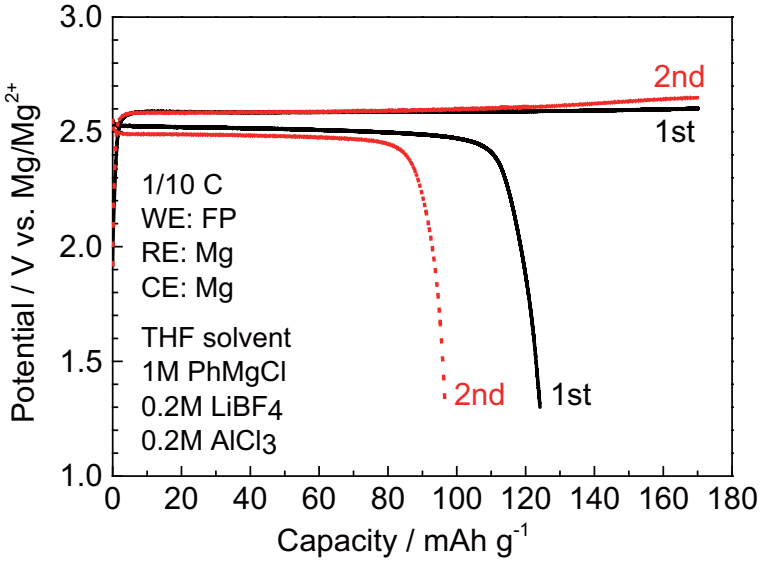

FIG. 5: Discharge-charge curves of fully delithiated $LiFePO_4$ ($FePO_4$) in the dual-salt THF electrolyte containing 1.0 M PhMgCl, 0.20 $MAlCl_3$, and 0.20 M $LiBF_4$. Cutoff condition: 1.3 V for discharge, charged electricity amount, 170 mAh g^{-1}.

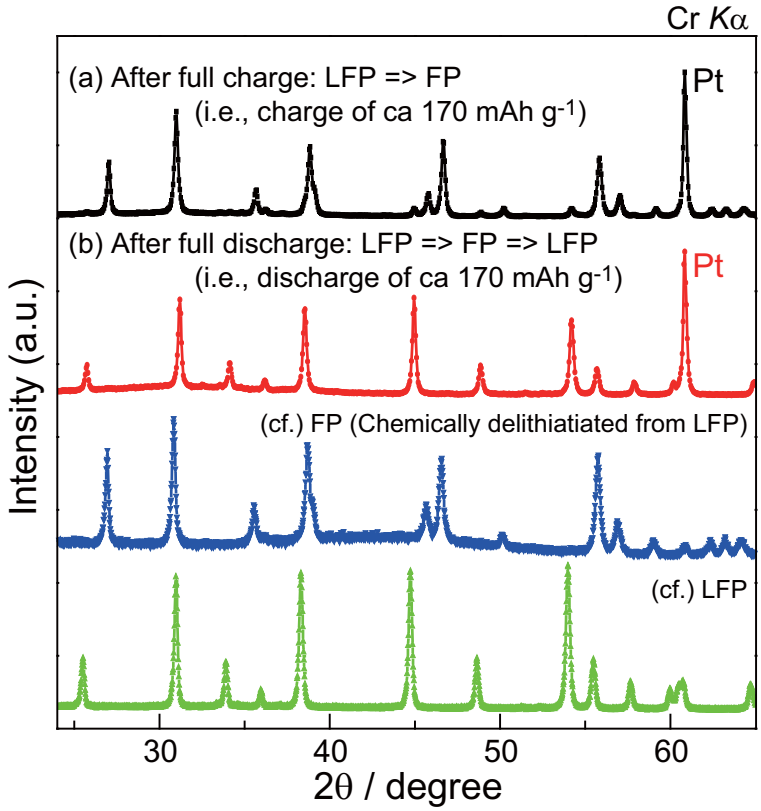

FIG. 6: XRD profiles measured after sufficient (a) charge and (b) discharge tests in the dual-salt THF electrolyte containing 1.0 M PhMgCl, 0.20 $MAlCl_3$, and 0.20 M $LiBF_4$.

Supplementary information: A concept of dual-salt polyvalent-metal storage battery

Shunsuke Yagi,[1] Tetsu Ichitsubo,[2,*] Yoshimasa Shirai,[2] Shingo Yanai,[2] Takayuki Doi,[3]
Kuniaki Murase,[2] Eiichiro Matsubara[2]
[1] *Nanoscience and Nanotechnology Research Center, Osaka Prefecture University, Osaka 599-8570, Japan*
[2] *Department of Materials Science and Engineering, Kyoto University, Kyoto 606-8501, Japan*
[3] *Department of Molecular Chemistry and Biochemistry, Doshisha University, Kyotanabe, Kyoto 610-0321, Japan*
[*] *Corresponding author: tichi@mtl.kyoto-u.ac.jp*

It would be interesting to know to what extent the energy density is retained or improved by substituting a non-noble polyvalent metal for graphite negative electrode of conventional lithium ion batteries (LIBs). In general, the accurate energy density calculation is difficult, because there are many factors to be considered for the calculation (e.g., the weights of metallic current collectors, separator, solvent etc, other than the two electrodes and electrolyte solute). For the dual-salt Daniel type batteries, we have considered the case where magnesium is used as a negative electrode, on the assumption that small amount of electrolyte (or solvent) is only required by using a saturated electrolyte with precipitated salts. Here we consider two kinds of the anion A, Cl^- and BF_4^-, for LiA and MgA_2 salts. SI Table I compares the expected capacities, *Emf*, energy densities of the conventional rocking-chair batteries and dual-salt Daniel type batteries. In this calculation, we have taken up the three intercalation-type positive electrode materials ($LiCoO_2$, $LiFePO_4$, and $LiMn_2O_4$), two conversion-type positive electrode materials (FeF_3 and CoF_3), and also $Mg_2Mo_6S_8$ positive electrode materials[4] for a rocking-chair type Mg battery. The energy densities of the dual-salt Daniel type batteries are found to be almost comparable to the LIBs with a graphite negative electrode when using intercalation-type positive electrode materials on the assumption that LiCl salt, existing as a precipitates in the small amount of saturated electrolyte, works as a Li^+ ion reservoir. The overall energy density (E_{P+N}) can be kept at a high value since the energy density of Mg (E_N) is significantly high; however, if we take a count of the electrolyte amount, the energy density is inevitably lowered.

SI Table I: Theoretical, actual capacities and expected energy densities for various combinations of positive and negative electrodes (PE and NE). The value of availability means the amount of Li (or Mg) that can be used without the decomposition of the active materials, and $C_{\rm the}$ and $C_{\rm act}$ mean the theoretical and actual ($C_{\rm act} = xC_{\rm the}$) capacities. $E_{\rm P}$ and $E_{\rm N}$ (given by $C_{\rm act} \times$ *Emf*) indicate the expected energy densities by using only positive electrode material, only negative electrode material, respectively, and $E_{\rm P+N}$ is the overall energy density of both electrode materials, where the underlined materials are defined as a positive active material for the calculation of $E_{\rm P}$. Note that the amount of electrolyte (or solvent) is not considered for the energy-density calculations. The *Emf* values are estimated on the basis of the data in literature.[20] The theoretical capacities of graphite (372 mAh g^{-1}) and Mg (2234 mAh g^{-1}) were used for the estimation of the energy densities.

Capacity and energy density	x	$C_{\rm the}$ mAh/g	$C_{\rm act}$ mAh/g	*Emf* V	$E_{\rm P}$ mWh/g	$E_{\rm N}$ mWh/g	$E_{\rm P+N}$ mWh/g
Rocking-chair type							
Intercalation reaction							
$Li_{1-x}CoO_2 + xLiC_6 = \underline{LiCoO_2} + 6xC$	0.6	274	164	3.7	608	1378	422
$Li_{1-x}FePO_4 + xLiC_6 = \underline{LiFePO_4} + 6xC$	1.0	170	170	3.1	527	1154	362
$Li_{1-x}Mn_2O_4 + xLiC_6 = \underline{LiMn_2O_4} + 6xC$	0.8	148	119	3.5	415	1303	315
$(1/2)Mg_{2(1-x)}Mo_6S_8 + xMg = (1/2)\underline{Mg_2Mo_6S_8} + 0$	1.0	122	122	1.2	146	2681	146
Conversion reaction							
$FeF_3 + 3LiC_6 = \underline{Fe + 3LiF} + 18C$	-	602	602	2.6	1565	968	598
$CoF_3 + 3LiC_6 = \underline{Co + 3LiF} + 18C$	-	588	588	3.3	1941	1229	752
Dual-salt Daniel type							
Intercalation reaction with LiCl							
$\underline{Li_{1-x}CoO_2 + xLiCl} + (1/2)xMg = LiCoO_2 + (1/2)xMgCl_2$	0.6	225	135	3.3	445	7372	420
$\underline{Li_{1-x}FePO_4 + xLiCl} + (1/2)xMg = LiFePO_4 + (1/2)xMgCl_2$	1.0	139	139	2.7	375	6031	353
$\underline{Li_{1-x}Mn_2O_4 + xLiCl} + (1/2)xMg = LiMn_2O_4 + (1/2)xMgCl_2$	0.8	128	103	3.1	318	6925	304
Intercalation reaction with $LiBF_4$							
$\underline{Li_{1-x}CoO_2 + xLiBF_4} + (1/2)xMg = LiCoO_2 + (1/2)xMg(BF_4)_2$	0.6	179	107	3.3	354	7372	338
$\underline{Li_{1-x}FePO_4 + xLiBF_4} + (1/2)xMg = LiFePO_4 + (1/2)xMg(BF_4)_2$	1.0	110	110	2.7	296	6031	282
$\underline{Li_{1-x}Mn_2O_4 + xLiBF_4} + (1/2)xMg = LiMn_2O_4 + (1/2)xMg(BF_4)_2$	0.8	107	86	3.1	266	6925	256
Conversion reaction with LiCl							
$\underline{FeF_3 + 3LiCl} + (3/2)Mg = 3LiF + Fe + (3/2)MgCl_2$	-	335	335	2.2	737	4914	641
$\underline{CoF_3 + 3LiCl} + (3/2)Mg = 3LiF + Co + (3/2)MgCl_2$	-	331	331	2.9	959	6478	835
Conversion reaction with $LiBF_4$							
$\underline{FeF_3 + 3LiBF_4} + (3/2)Mg = 3LiF + Fe + (3/2)Mg(BF_4)_2$	-	204	204	2.2	449	4914	411
$\underline{CoF_3 + 3LiBF_4} + (3/2)Mg = 3LiF + Co + (3/2)Mg(BF_4)_2$	-	202	202	2.9	587	6478	538